Ab Initio calculation of the thermal neutron scattering cross sections of uranium mononitride

Wang Lipeng[1) 2)] Jiang Xinbiao [1)] Wu Hongchun [2)] Fan Huiqing [3)]

1) (State Key Lab of Intense Pulsed Radiation Simulation and Effect, Northwest Institute of Nuclear Technology, Xi'an, 710024, China)

2) (School of Nuclear Science and Technology, Xi'an Jiao Tong University ,Xi'an, 710049, China)

3) (State Key Laboratory of Solidification Processing, School of Materials Science and Engineering, Northwestern Polytechnical University, Xi'an 710072, China)

ISINN26
May 28 to June 1 2018 Xi'an China

Contents

- **Introduction**
  - Purpose; Why; What; How
- **Calculations**
  - Theory; Tools
- **Results**
  - Figures; Tables; Data analysis
- **Conclusions**
  - Conclude; Evaluations; Prospect

Introduction

Compared with UO_2 fuel, UN has higher uranium density, higher melting point, higher thermal conductivity, lower thermal expansion coefficient, and more stability in irradiation as well as less fission gas release. It was chosen as a promising potential material for advanced power reactor and a new concept of Accident Tolerance Fuel. Thermal reactor design and analysis need more reliable thermal neutron scattering cross sections in order to calculate accurate physical parameters in reactor core because thermal neutron cross sections have a great impact on neutronic criticality and neutron spectrum.

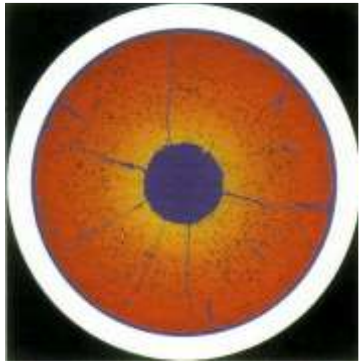

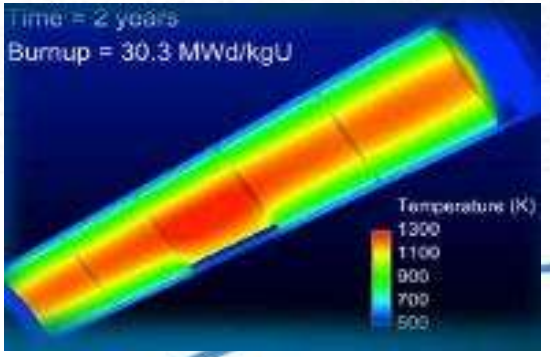

Introduction

- Former thermal neutron scattering cross section library only provide traditional UO_2 fuel thermal neutron scattering cross section, e.g. ENDF70SAB libraries in MCNP5. No thermal library for UN is available, which would bring big errors in calculations of reactor physics for advanced LWRs or other thermal reactors used UN as fuels. Thermal neutron scattering cross sections of UN fuel were needed to be studied.
- The calculation of the thermal neutron scattering cross sections requires a detailed knowledge of the lattice dynamics of the scattering medium. The vibrational properties of UN should be studied. Generally, thermal neutron scattering cross sections were represented as thermal scattering law $S(\alpha,\beta)$. ENDF Library was setting TSL File to describe it. Specified evaluated nuclear data library just only provided several moderator materials. As for thermal neutron scattering cross sections of UN, reliable method of processing thermal neutron scattering cross sections should be investigated.

Introduction

- Thermal Neutron Scattering Theory

Inelastic scatterings: $$\frac{d^2\sigma}{d\Omega dE'}(E\to E',\mu,T)=\frac{\sigma_b}{4\pi kT}\left(\frac{E'}{E}\right)^{0.5}\exp\left(-\frac{\beta}{2}\right)S(\alpha,\beta,T)$$

$$S(\alpha,\beta)=\frac{1}{2\pi}\int_{-\infty}^{+\infty}e^{i\beta t}e^{-\gamma(t)}dt,\gamma(t)=\alpha\int_{-\infty}^{+\infty}\frac{\rho(\beta)}{2\beta\sinh(\beta/2)}[1-e^{i\beta t}]e^{-\beta/2}d\beta$$

$$\alpha=\frac{E'+E-2\sqrt{E'E}\cos\theta}{AkT}=\frac{\hbar}{2MkT}\qquad\beta=\frac{E'-E}{kT}=\frac{\varepsilon}{kT}$$

Elastic scatterings: $$\frac{d^2\sigma}{d\Omega dE'}=\frac{\sigma_b}{4\pi}\exp(-2E(1-\mu)\frac{\gamma(0)}{A})\delta(\mu)\delta(E-E')$$

$$\frac{\mathrm{d}^2\sigma_{coh}}{\mathrm{d}\Omega\mathrm{d}E'}=\frac{\sigma_b}{E}\sum_{E_i<E}f_i e^{-4\gamma(0)\mathrm{Ei/A}}\delta(\mu-\mu_i)\delta(E-E')$$

Debye Wall Integral： $$\gamma(0)=\int_0^{\omega_{\max}}\frac{\rho(\omega)}{\hbar}\coth\frac{\hbar}{2kT}a\omega$$

Effective temp： $$T_{eff}=\frac{1}{2}\int_0^{\omega_{\max}}\hbar\qquad\frac{\hbar}{2kT}\rho(\omega)a'\omega$$

Introduction

- Thermal Neutron Scattering Theory
  - Obtaining the phonon data, the inelastic thermal neutron scattering cross sections were generated, using the NJOY code system, at different temperature. The theory is exposed in details in many books and report [5-7]. For the UN, the incoherent approximation and Gaussian approximation were used

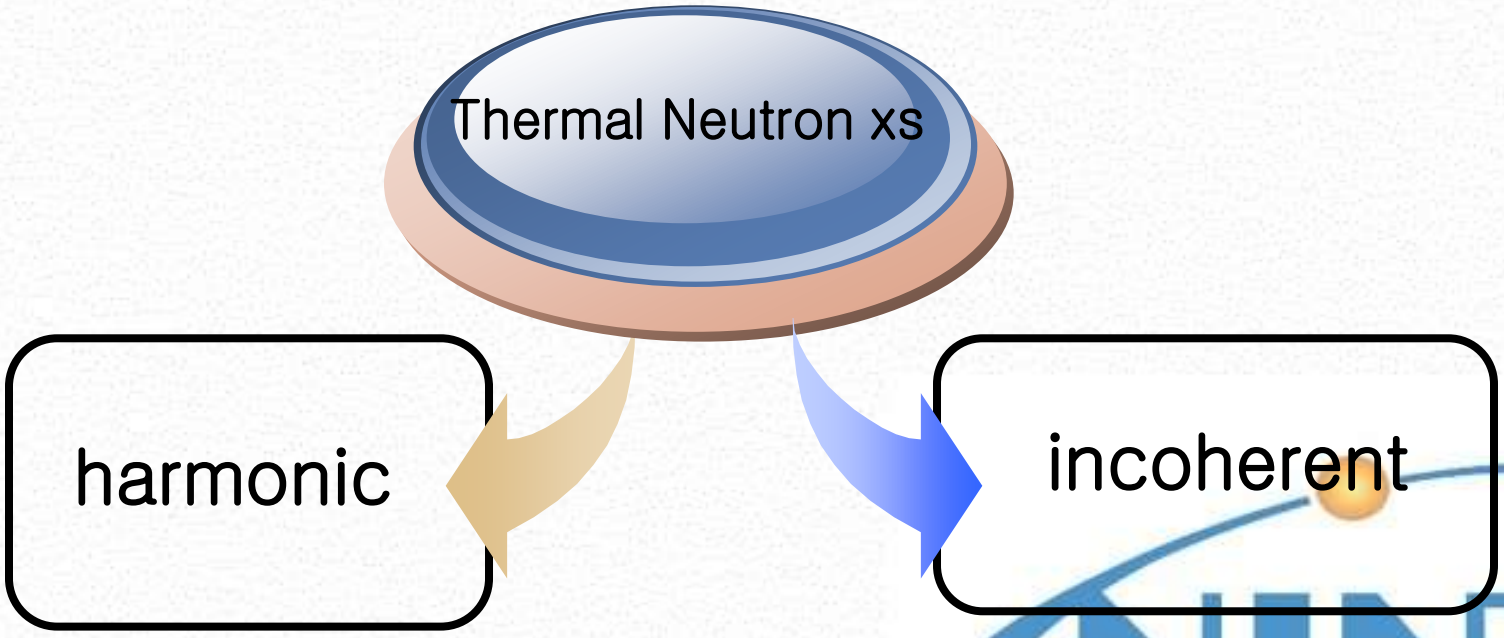

Calculation

Ab Initio and Phonon calculation

- Atom structure of uranium nitride is listed in Fig.1, which is similar with NaCl, KCl, and MgO structure, called Faced Centered Cubic structure, primitive cell only contains two atoms, and each atom is surrounded by other six atoms.
- MedeA platform of Material Design was used in this calculation. Phonon dispersions and phonon density of states was calculated by utilizing VASP and PHONON code. GGA potential functions was chosen, cutoff energy was 400 eV, super cell lattice method was used in 6×6×6 Monk host-Pack grid, The phonon frequency distributions were determined from Hellmann-Feynman forces where these forces were computed from four independent.

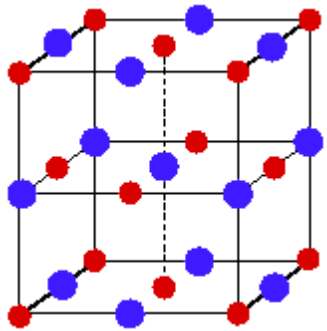

materials design

Predict with MedeA®

Calculation

- Ab Initio and Phonon calculation

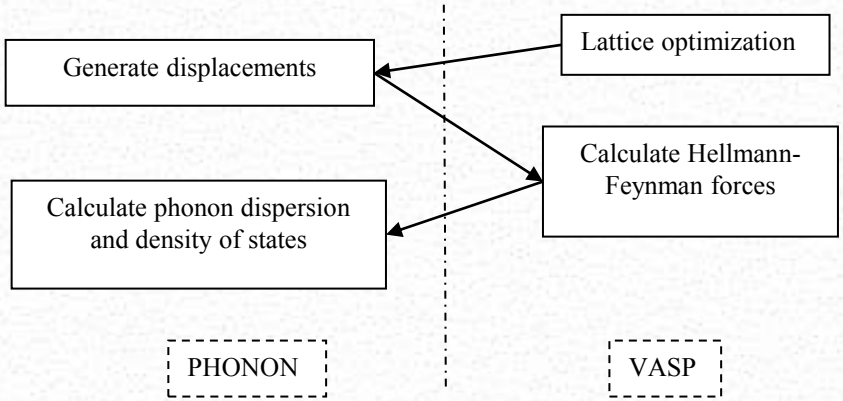

The flowchart

To validate the accuracy of phonon spectrum, the heat capacity of UN which is integral of phonon density of states was calculated in order to compare with experimental ones. The heat capacity can be expressed:

$$C = rk_B \int_0^{\infty} d\omega \rho(\omega) \left(\frac{\hbar}{k_B T} \right)^2 \frac{e^{\left(\frac{\hbar}{k_B T} \right)}}{\left(e^{\left(\frac{\hbar}{k_B T} \right)} - 1 \right)^2}$$

Calculation

- Ab Initio and Phonon calculation
  - Because N-14 has relative thermal neutron absorption cross sections, and the product C-14 has long half-life. In practice, higher content of $U^{15}N$ was used, other parameters were consistent with UO_2, which treated U as U-238, Table 1 listed different bound cross sections of isotopes in UN, and the free atom cross section was expressed:

$$\sigma_{\text{free}} = \left(\frac{A}{A+1}\right)^2 \sigma_{\text{b}}$$

Atom	AWR	σ_a	σ_{coh}	σ_{inc}	σ_b	σ_{free}
U-238	236.0058	2.68	8.871	0	8.871	8.7963
N-14	13.88278	1.91	11.03	0.5	11.53	10.036
N-15	14.87100	0.000024	5.21	0.00005	5.21	4.5714

Results

Lattice parameters

- Structure optimization of UN was done using VASP code, initial parameters adopted values in Pearson Library, and convergence criterion was set to 1e-5 eV, cutoff energy was 400 eV, GGA and LDA potential were used to calculate. Results were shown in Table.2, which revealed that GGA was better than LDA to get closer to experimental values.

Methods	GGA	LDA	Pearson
a=b=c	4.841841	4.775800	4.890000
Error	-1.0%	-2.3%	-

Results

- Phonon spectrum
  - The phonon dispersion relationships at different directions in Brillion zone were listed in Fig.3. The low branch is acoustic part, causing by heavy atom U, while the high branch is optic part, causing by light atom N. The derived phonon density of states and compared results with UO_2 were listed in Fig.4-6, two parts separated well.

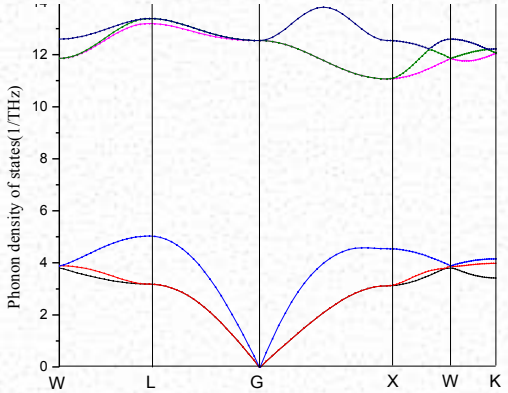

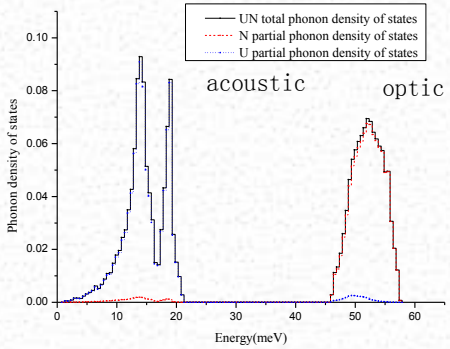

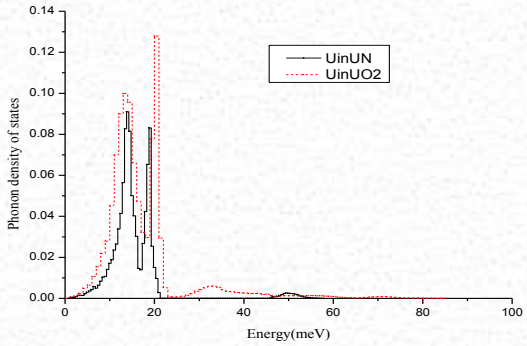

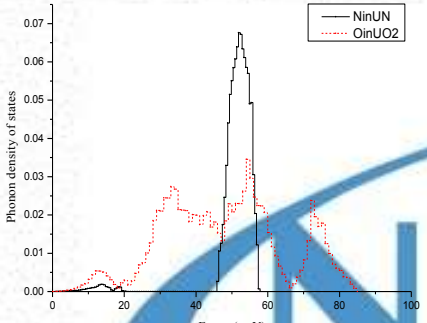

Results

- Heat capacity of UN

  - Fig.7 listed the changes of heat capacity of UN with temperature, and compared with MD results. As can be seen, Cv calculated in this paper was closer to experimental ones, therefore the generated phonon density of states was accurate.

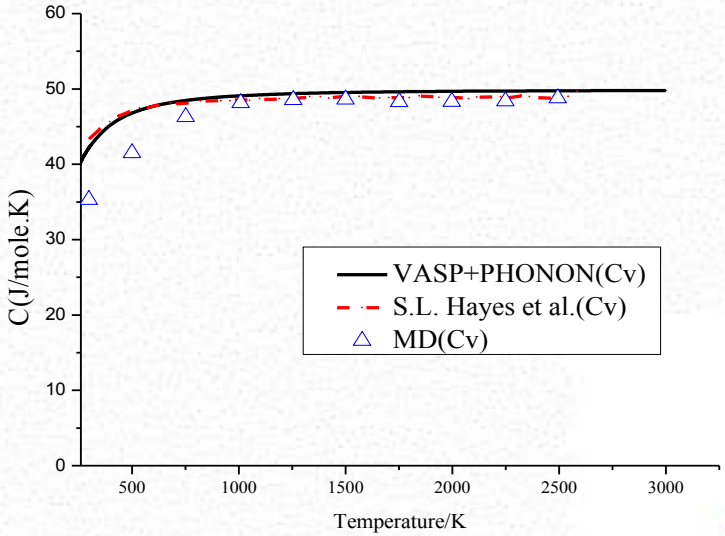

Results

S(α,β) of UN

- Changes of S(α,β) of N in UN and U in UN were shown in Fig.8, and α=0.5, α=1.33 and α=10 results were listed, as can be seen, when α values is small, S(α,β) changed a lot by β, which is caused by phonon spectrum effect. After α values become higher, vibration effect is low, and this circumstance of U in UN is not obvious in case of heavy U atom, there is no need to expand β.

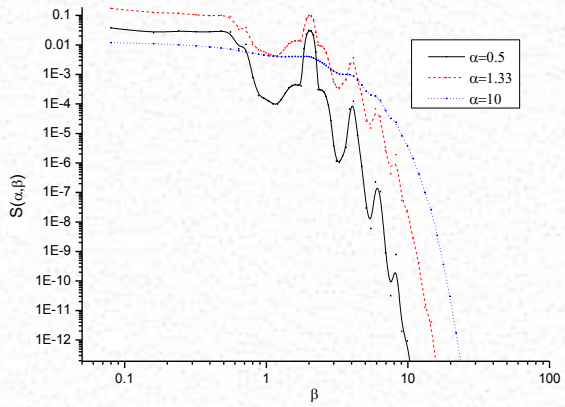

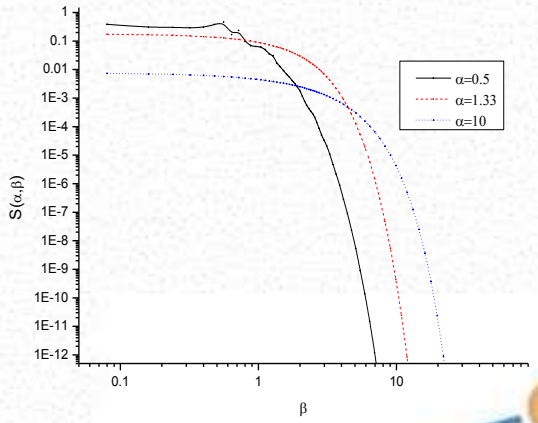

Results

Debye Waller integral and T_{eff}

- From equations (8)~(10), SCT approximation was used when energy is outside S(α,β), the inelastic scattering is decided by T_{eff}, while from equations (11)~(16), incoherent elastic cross section was decided by γ(0). Table 3 listed the Debye Waller integral and T_{eff} parameters

Temp/K	U-238		N-14(N-15)	
	Debye Waller Integral /eV-1	Teff /K	Debye Waller Integral /eV-1	Teff /K
293.6	9.200004	304.01	0.977924	387.84
400.0	16.935232	407.71	1.685904	471.25
500.0	26.368138	506.19	2.545795	557.74
600.0	37.897091	605.17	3.595424	648.47
700.0	51.522145	704.44	4.835249	741.73
800.0	67.243324	803.89	6.265468	836.61
1000.0	104.974093	1003.11	9.697441	1029.39
1200.0	151.089438	1202.60	13.891709	1224.54

Results

- Thermal scattering cross sections

  - In order to see the distinction between UO2 and UN, comparison between O-16, U-238 in UO2 and N-15(N-14), and U-238 in UN in inelastic and elastic cross sections at 293.6 K were listed in Fig.9. Fig.10. listed the changes from inelastic and elastic cross sections of N in UN and U in UN with temperatures. As can be seen, O-16 in UO_2 consider coherent elastic part. N-14 and N-15 in UN neglected coherent elastic part, and inelastic cross sections of N-14 were a little higher than N-15, inelastic cross sections of N-14 were closer to O-16. The inelastic and elastic cross sections of U-238 in UN is less than U-238 in UO2, and with the temperature increasing, the inelastic cross sections of N in UN and U in UN increase, and the elastic cross sections decrease. Total cross sections mainly come from inelastic part, and equal to free atom cross section when energy is larger than 1 eV.

Results

- Thermal scattering cross sections

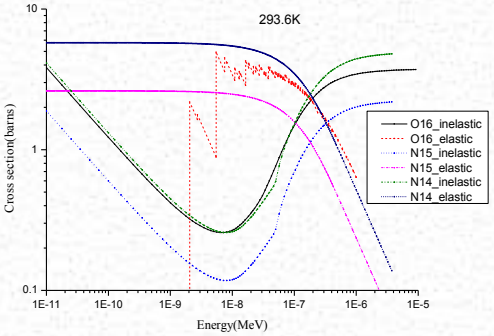

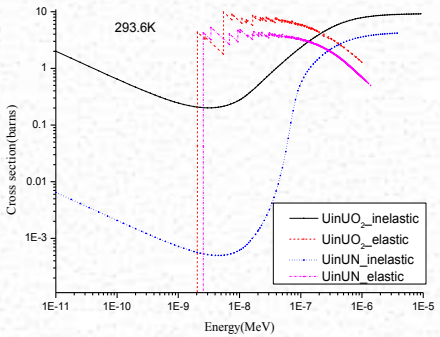

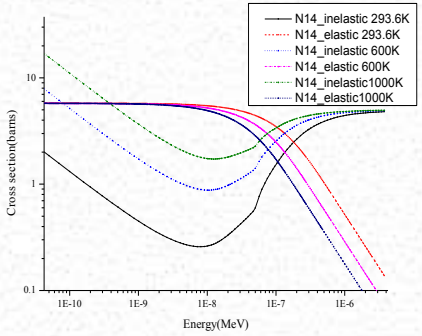

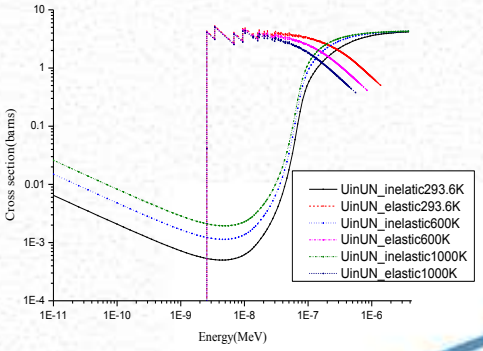

Conclusions

- This paper generated thermal neutron scattering cross sections of UN using ab intio method based on thermal scattering theory. Results indicated that optimized lattice parameter reached good agreement with data base; the optical modes were well separated from the acoustic modes compared with UO_2; heat capacity at a constant volume was consistent with experimental value; the inelastic and elastic cross sections of U-238 in UN were lower than those of U-238 in UO2 calculated by this phonon spectrum. N in UN only dealt with incoherent part in elastic cross sections. As the temperature increased, elastic cross sections of UN decreased and inelastic ones increased, and approached to free atom cross sections in high energies. This paper's conclusion could fulfill the vacancy of thermal neutron scattering cross sections of UN, which laid a foundation for systematic study on neutronics of UN fuel in LWRs.

Thanks for your listening!

ISINN26
May 28 to June 1 2018 Xi'an China